JACS
JOURNAL OF THE AMERICAN CHEMICAL SOCIETY

COMMUNICATION

pubs.acs.org/JACS

Synthesis and Characterization of Wurtzite ZnTe Nanorods with Controllable Aspect Ratios

Jun Zhang,*[,†] Shengye Jin,[†,‡] H. Christopher Fry,[†] Sheng Peng,[†] Elena Shevchenko,[†] Gary P. Wiederrecht,[†,‡] and Tijana Rajh*[,†]

[†]Center for Nanoscale Materials, Argonne National Laboratory, Argonne, Illinois 60439, United States

[‡]Argonne-Northwestern Solar Energy Research (ANSER) Center, Northwestern University, Evanston, Illinois 60208, United States

Supporting Information

ABSTRACT: ZnTe nanorods with controllable aspect ratios were synthesized using polytellurides a tellurium precursor. The use of polytellurides which allow nucleation and growth at relatively low temperature is the key to formation of wurtzite phase and controlled anisotropic growth along *c*-axis. The aspect ratio of the resulting ZnTe nanorods was controlled by tuning the temperature that in turn controls the kinetics of the nanocrystal growth. A diameter dependent quantum confinement effect in ZnTe nanorods was observed by UV−vis absorption spectroscopy. Transient absorption measurements show ultrafast charge injection dynamics from ZnTe nanorods, suggesting their strong potential for applications in photocatalysis.

One-dimensional (1D) semiconductor nanocrystals (NCs) are of great interest for both fundamental research and technical applications, due to their unique optical and electronic properties.[1−4] Zinc telluride (ZnTe) is a very attractive semiconductor that has applications in blue-green light-emitting diodes,[5] electro-optic detectors,[6] and solar cells.[7] In particular, compared to many other semiconductors, ZnTe possesses a more negative conduction band edge position (−1.7 V vs NHE),[8] which leads to a large driving force for interfacial electron transfer from semiconductor to electron acceptors.[8] As a result, ZnTe can be a very promising candidate for improving the solar to electric power conversion efficiency in solar cells and designing novel photocatalysts. Although ZnTe nanostructures have been prepared through various approaches,[9−18] it is still a challenge to achieve synthesis of high-quality ZnTe 1D NCs with finely tuned aspect ratios. In fact, the major issue in preparing ZnTe NCs is the lack of suitable precursors for controlling the thermodynamics and kinetics of the nanocrystal nucleation stage,[15,19] which is essential for controlling of the size and shape of the resulting NCs. In addition, crystal symmetry is known to influence the optoelectronic properties of semiconductor NCs,[20,21] and it would be of great interest to develop a kinetically controlled synthesis of unusual metastable crystal phases.

The precursor injection method, which features the separation of the nanocrystal nucleation and growth stages, has been widely used for the preparation of many types of metal telluride NCs.[22,23] However, a similar method involving the fast injection of tellurium-trioctylphosphine (Te(TOP)), which is the most commonly used Te precursor, only provided limited control over the size and shape of the resulting ZnTe NCs.[12,15] In this communication, we demonstrate a facile strategy in preparation of ZnTe nanorods (NRs) with controllable aspect ratios, using polytellurides as a tellurium (Te) precursor. In contrast to previous reports, this method yields ZnTe NRs with a hexagonal wurtzite (WZ) structure, which is less thermodynamically stable than the commonly observed cubic zinc blende (ZB) structure,[24] and has rarely been reported for ZnTe in the nanocrystalline regime.[16]

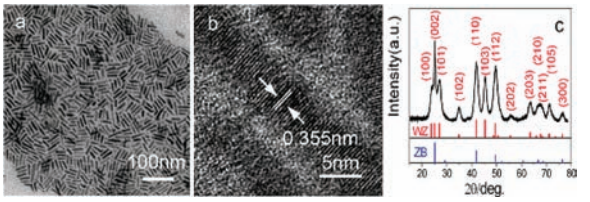

Figure 1. (a) TEM image, (b) HRTEM image, (c) X-ray diffraction pattern of ZnTe NCs synthesized at 300 °C. The standard XRD patterns of ZB and WZ structured ZnTe are also present in panel (c) for comparison.

Previously, TeH^- anions which were prepared by reducing Te(TOP) with superhydride were used to synthesize ZnTe NCs.[15] However, this method provided very limited growth control. In our new strategy, the Te precursor was prepared by mixing Te(TOP), superhydride and oleylamine under nitrogen (Figure S1). The UV−vis absorption and mass spectrum (Figures S2−S3) of the Te precursor confirm the presence of a mixture of Te^{2-}, Te_2^{2-}, Te_3^{2-} and even a small amount of higher polytellurides.[25,26] The freshly prepared Te precursor was immediately injected into a zinc solution preheated to 160 °C. After the nucleation stage, the system was heated to high temperatures (190−300 °C) and kept for a period of time ranging from 20 to 90 min for crystal growth. The resulting ZnTe NCs were separated by precipitation and centrifugation (Supporting Information for details).

Figures 1−3 present overview micrographs of ZnTe NCs synthesized under different reaction conditions. High-resolution transmission electron microscopy (HRTEM) observation (Figure 1b) reveals lattice fringes corresponding to a spacing of 0.355 nm, that matches well with the expected *d*-spacing of the

Received: July 25, 2011
Published: September 07, 2011

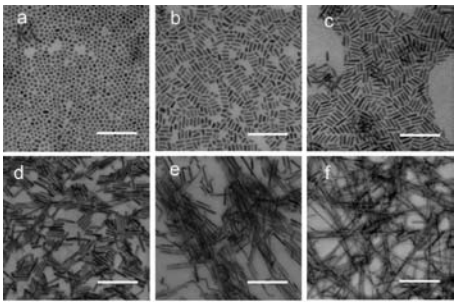

Figure 2. TEM images of ZnTe NCs with dimensions of (a)7.0 ± 0.7 nm, (b) 21.5 ± 4.9 nm × 6.8 ± 0.4 nm, (c) 31.0 ± 7.0 nm × 6.9 ± 0.6 nm, (d) 40.9 ± 8.4 nm×x 6.9 ± 0.5 nm, (e) 88.6 ± 33.9 nm × 6.8 ± 0.7 nm, and (f) 140.1 ± 42.1 nm × 6.8 ± 0.6 nm . Bars are 100 nm.

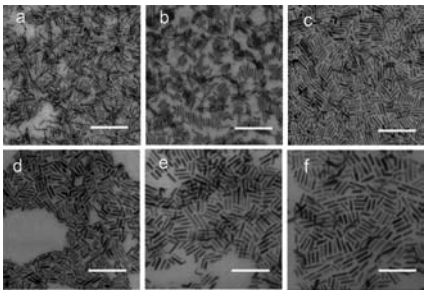

Figure 3. TEM images of ZnTe NCs with various sizes grown at different temperatures: (a) 190 °C (30.9 ± 6.5 nm × 3.5 ± 0.3 nm), (b) 220 °C (30.2 ± 5.8 nm × 4.1 ± 0.45 nm), (c) 240 °C (29.9 ± 7.2 nm × 5.2 ± 0.44 nm), (d) 260 °C(30.6 ± 8.7 nm × 5.9 ± 0.60 nm), (e) 280 °C (31.6 ± 5.3 nm × 6.4 ± 0.67 nm), and (f) 300 °C (31.9 ± 5.0 nm × 7.0 ± 1.3 nm). Bars are 100 nm.

(002) plane of the WZ structure of ZnTe. According to the energy-dispersive X-ray (EDX) spectroscopy data (Figure S4), the Zn/Te atomic ratio is close to a 1:1 stoichiometry. X-ray powder diffraction (XRD) analysis (Figure 1c) confirms the WZ structure of ZnTe [space group *P*63*mc*] (JCPDS card 19-1482). Among all reflection peaks, the (002) peak is more intense and narrower indicating preferential growth of ZnTe along the *c*-axis.

Many II−VI semiconductors such as ZnS, ZnSe, ZnTe, and CdTe have both ZB and WZ structures, and the bulk ZB structure is energetically more favorable than that of WZ.[24,27−29] However, due to low surface energy and small surface stress in the nanocrystalline regime, WZ phase can be obtained at the nanoscale.[30] Despite the fact that NCs of many II−VI semiconductors such as CdSe, CdTe, ZnS, and ZnSe have been prepared in both forms, there are only a few reports of synthesis of WZ ZnTe nanostructures.[16] Nevertheless, it has been shown theoretically that the phase transition can occur in ZnTe smaller than 7.0 nm.[30] Thus, the ability of polytellurides to initiate nucleation and growth of ZnTe NCs in a temperature range where the energy difference between phases, ZB and WZ, is still significant, is a key point of our approach. As evidence, we conducted a control experiment by injecting the telluride precursor at an elevated temperature, 230 °C. As expected, we observed the presence of ZB reflection peaks for the resultant sample. When the injection temperature was further increased to 250 °C, the majority product of the resulting nanoparticles was of ZB phase. (Figure S5) Alternatively, a low precursor injection temperature (160 °C) followed by a high growth temperature (300 °C) resulted in WZ phase instead of ZB phase, suggesting the phase of the final ZnTe NCs was determined by the original phase of nucleates.

A control experiment revealed that the ZnTe NCs could only form at high temperatures (e.g. >250 °C) when a Te(TOP) solution without superhydride was injected into a zinc precursor solution, yielding ZnTe (ZB phase) nanoparticles with poorly defined morphologies (Figure S6). However, the adoption of polytellurides as a Te precursor allows a much lower nucleation temperature (∼160 °C), leading to the separation of successive NC growth at higher temperatures from the initial nucleation stage. In contrast, the high chemical reactivity of the precursor also leads to extremely high concentration of monomer, which favors the kinetic growth, as required for the anisotropic growth of NCs with WZ structures.[31] To investigate the growth mechanism of ZnTe NCs, aliquots were taken for TEM observation (Figure S7), as the reaction temperature was steadily increased to 300 °C at a rate of 10 °C/min after Te precursor injection at 160 °C. It was found that the NC growth was sustained during the entire process as the temperature was increased from 160 to 300 °C. The anisotropic 1D growth trend was observed for samples taken at 180 °C and above. Previous studies show the significantly higher surface energy of the $(00\bar{1})$ of the WZ crystal structure in CdSe systems, compared to the other facets, resulting in the formation of 1D structures.[31−33] In our synthesis, the particular reaction conditions combined with active Te precursor ensured the selective growth on the high energy $(00\bar{1})$ facet,[15] leading to successful anisotropic growth. As a characteristic of the anisotropic growth mechanism, a relatively high concentration of the precursor is required for nanorod formation.[34] Indeed, reagent concentration plays an important role in the 1D ZnTe NC growth. When the amount of reactants was decreased by one-half while maintaining all other conditions, quasi-spherical ZnTe NCs (Figure 2a) were obtained instead of the anisotropic 1D structure.

Further studies revealed that the molar ratio between Te(TOP) and superhydride significantly affects the shape of the resulting ZnTe NCs, suggesting the presence of several active Te species formed upon reduction of Te(TOP) by superhydride that participate in the growth of ZnTe NRs (Figure S8). When pure Te(TOP) was introduced into a zinc solution at 190 °C, no NCs were formed indicating that Te(TOP) is not active at this temperature. Similarly, when a mixture of Te(TOP) with a small amount (0.1 mL) of superhydride was added to the Zn solution at the same temperature, a small amount of irregular shaped NCs were obtained. However, when Te(TOP) was converted into the highly reactive polytelluride species using approximately equimolar amounts of superhydride in the presence of oleylamine, well-defined ZnTe NRs with a diameter of 3.5 nm formed at 190 °C. Further increase of the amount of superhydride resulted in complete conversion of polytelluride into monomeric Te^{2-}, and consequently, we observe formation of the mixture of small aspect ratio NRs and NCs with diameters of ∼3.5 nm. On the basis of the above observations, we believe that at low temperatures (160−190 °C), polytellurides and Te^{2-} are both active tellurium species that participate in the NC growth at low temperatures; however, their activity[35] and, consequently, the mechanism of particle growth they support are very different. While monomeric Te^{2-} is highly active, it promotes growth with little selectivity of facets, polytellurides react much more slowly and are able to react only with the highly active $(00\bar{1})$ facet, promoting the growth of the 1D structure. When the temperature is increased (≥300 °C), less active elemental Te starts to participate in growth,

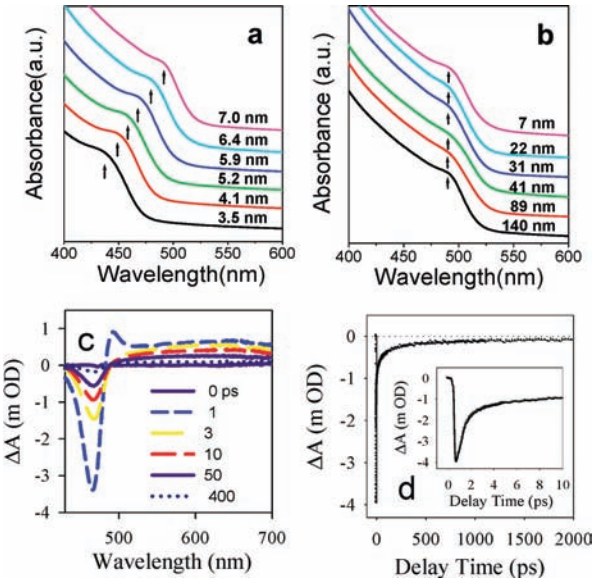

Figure 4. (a) Absorption spectra of ZnTe nanorods of various diameters with similar lengths (~30 nm). (b) Absorption spectra of 7 nm diameter ZnTe nanorods with various lengths. (c) TA spectra of ZnTe nanorods at several delay times (on a picosecond time scale) following 410 nm excitation (~30 nJ/pulse). (d) TA kinetics of ZnTe nanorods probed at the exciton bleach at 465 nm. The inset shows the kinetics at early delay times.

leading to the increase of the length of ZnTe NCs, due to the selective growth of the high energy facet $(00\bar{1})$. By simply increasing the growth time at 300 °C, ZnTe NCs were found to increase in length from approximately 20−80 nm (Figure 2b−e) indicating a direct correlation between length and time. The average length of ZnTe NCs could be further elongated to about 140 nm (Figure 2f) by increasing the Zn/Te precursor input ratio to 2:1, in addition to a 60 min growth time at 300 °C.(Supporting Information) Despite the various lengths, those NCs grown at 300 °C have a similar width of ~7 nm.

The solid/liquid ratios (mg/mL) of aliquots corresponding to these NCs were also calculated (Table S1). By comparison, it was found that solid/liquid ratios have a roughly linear dependence on the average volume of a single nanorod. This provides a strong hint that increasing the nanorod dimension resulted from continuous crystal growth, instead of digestion of the smaller NCs present in the reaction solution.

Tuning the width of ZnTe NRs was realized by controlling the growth kinetics, in which the growth temperature was increased from 160 to 300 °C in a stepwise mode (Supporting Information). For instance, a growth at 190 °C for 60 min led to the formation of ZnTe NCs with an average dimension of 30.9 nm long and 3.5 nm wide (Figure 3a). After the initial 60 °C growth at 190 °C, the reaction temperature was elevated (220, 240, 260, 280, and 300 °C respectively) and kept at each temperature for an additional 60 min, where ZnTe NCs with average width of 4.1, 5.2, 5.9, 6.4, and 7.0 nm could be obtained with no obvious increase in length.(Figure 3b−f) We believe that the control of NR diameter is obtained by altering dissociation equilibrium of polytellurides (Te_2^{2-} and Te_3^{2-}) at different temperatures. Raising the temperature (190 °C < T < 300 °C) shifts the equilibrium toward dissociated Te^{2-} and elemental Te, increasing the concentration of highly reactive Te^{2-} that enables growth of less active facets and therefore NR diameter.

To characterize the optical properties of the NCs, we measured their absorption and photoluminescence features. Figure 4a shows UV−vis absorption spectra of ZnTe nanorod samples with various diameters. As displayed, all the samples show a distinguishable absorption peak which progressively shifts to longer wavelength as the nanorod diameter increases. Compared with the position of the 548 nm (2.26 eV)[36] absorption band edge of bulk ZnTe, an obvious confinement effect was observed for all ZnTe nanorod samples. The absorption spectra of ZnTe NCs of the same width (7 nm), but with various lengths (shown in Figure 2a−e), were also studied. As presented in Figure 4b, all the samples show absorption peaks at almost the same position (~480 nm), regardless of the different lengths. These findings suggested that the blue shift of absorption peaks of these ZnTe NCs was attributed to the quantum confinement resulting from the small diameters of the ZnTe NCs rather than their length.[31,37] Consistent with many previous reports,[12,38,39] no photoluminescence was observed from ZnTe NCs.

To further corroborate the lack of photoluminescence, the exciton dynamics of one set of ZnTe nanorod samples (30 nm × 5.2 nm) was examined by ultrafast transient absorption (TA) spectroscopy. The TA spectra (Figure 4c) and kinetics (Figure 4d) show that the excitons in the ZnTe nanorods monitored at 465 nm are very short-lived, on the order of a few picoseconds. The longer-lived kinetic components (after 4 ps) are likely due to charge-separated states.[40] The broad spectral feature on the red side of the exciton is assigned to the creation of long-lived holes in semiconductor NCs,[41] offering further evidence for the presence of a longer-lived charge separated state. The short exciton lifetime is probably due to electron injection into surrounding accepting states, as a consequence of the high reducing power of ZnTe.[39] Further studies on the transient absorption of ZnTe NCs are underway.

In summary, we developed a facile synthetic approach for producing high-quality WZ ZnTe NCs with controlled aspect ratio by adoption of active polytellurides as a tellurium precursor in conjunction with varying precursor concentration, reaction temperature, and/or reaction time. UV−vis absorption spectra confirm that the NCs possess obvious quantum confinement effects. TA measurements show ultrafast charge injection dynamics from ZnTe nanorods, suggesting their strong potential for applications in photocatalysis.

■ ASSOCIATED CONTENT

Supporting Information. Experimental details about the synthesis and characterization of ZnTe nanorods; photograph, UV−vis absorption and MS spectrum of tellurium precursor. XRD and EDS spectrum of ZnTe nanorods; TEM images of ZnTe NCs synthesized under different conditions. This material is available free of charge via the Internet at http://pubs.acs.org.

■ AUTHOR INFORMATION

Corresponding Author
junzhang@anl.gov; rajh@anl.gov

■ ACKNOWLEDGMENT

This work and the use of the Center for Nanoscale Materials were supported by the U.S. Department of Energy, US DOE-BES, under Contract No. DE-AC02-06CH11357. J.Z. acknowledges

the support from the Center for Nanoscale Materials at Argonne National Laboratory through a CNM distinguished postdoctoral fellowship. S.J. and G.P.W. acknowledge support for the ultrafast spectroscopy work as part of the ANSER Center, an Energy Frontier Research Center funded by the US Department of Energy, Office of Science, Office of Basic Energy Sciences (award No.DE-SC0001059). We thank Dr. Yugang Sun for the helpful discussion. We also acknowledge Professor Dmitri V. Talapin and Mr. Wenyong Liu for their help with XRD.

REFERENCES

(1) Li, J.; Wang *Nano Lett.* **2002**, *3* (1), 101.
(2) Li, L.-s.; Hu, J.; Yang, W.; Alivisatos, A. P. *Nano Lett.* **2001**, *1* (7), 349.
(3) Yu, P.; Nedeljkovic, J. M.; Ahrenkiel, P. A.; Ellingson, R. J.; Nozik, A. J. *Nano Lett.* **2004**, *4* (6), 1089.
(4) Jie, J.; Zhang, W.; Bello, I.; Lee, C.-S.; Lee, S.-T. *Nano Today* **2010**, *5* (4), 313.
(5) Tanaka, T.; Saito, K.; Nishio, M.; Guo, Q.; Ogawa, H. *Appl. Phys. Express* **2009**, *2* (12), 122101.
(6) Wu, Q.; Litz, M.; Zhang, X. C. *Appl. Phys. Lett.* **1996**, *68* (21), 2924.
(7) Schrier, J.; Demchenko, D. O.; Wang; Alivisatos, A. P. *Nano Lett.* **2007**, *7* (8), 2377.
(8) Kaniyankandy, S.; Rawalekar, S.; Verma, S.; Ghosh, H. N. *J. Phys. Chem. C* **2011**, *115* (5), 1428.
(9) Li, Y.; Ding, Y.; Wang, Z. *Adv. Mater.* **1999**, *11* (10), 847.
(10) Jun, Y.-w.; Choi, C.-S.; Cheon, J. *Chem. Commun.* **2001**, No. 1, 101.
(11) Du, J.; Xu, L.; Zou, G.; Chai, L.; Qian, Y. *J. Cryst. Growth* **2006**, *291* (1), 183.
(12) Lee, S. H.; Kim, Y. J.; Park, J. *Chem. Mater.* **2007**, *19* (19), 4670.
(13) Yong, K.-T.; Sahoo, Y.; Zeng, H.; Swihart, M. T.; Minter, J. R.; Prasad, P. N. *Chem. Mater.* **2007**, *19* (17), 4108.
(14) Fanfair, D. D.; Korgel, B. A. *Cryst. Growth Des.* **2008**, *8* (9), 3246.
(15) Zhang, J.; Sun, K.; Kumbhar, A.; Fang, J. *J. Phys. Chem. C* **2008**, *112* (14), 5454.
(16) Xu, S.; Wang, C.; Xu, Q.; Zhang, H.; Li, R.; Shao, H.; Lei, W.; Cui, Y. *Chem. Mater.* **2010**, *22* (21), 5838.
(17) Li, L.; Yang, Y.; Huang, X.; Li, G.; Zhang, L. *J. Phys. Chem. B* **2005**, *109* (25), 12394.
(18) Zhang, J.; Chen, P.-C.; Shen, G.; He, J.; Kumbhar, A.; Zhou, C.; Fang, J. *Angew. Chem.* **2008**, *120* (49), 9611.
(19) Jiang, F.; Li, Y.; Ye, M.; Fan, L.; Ding, Y.; Li, Y. *Chem. Mater.* **2010**, *22* (16), 4632.
(20) Viswanatha, R.; Sapra, S.; Saha-Dasgupta, T.; Sarma, D. D. *Phys. Lett. B* **2005**, *72* (4), 045333.
(21) Yang, Y. A.; Wu, H.; Williams, K. R.; Cao, Y. C. *Angew. Chem., Int. Ed.* **2005**, *44* (41), 6712.
(22) de Mello Donegá, C.; Liljeroth, P.; Vanmaekelbergh, D. *Small* **2005**, *1* (12), 1152.
(23) Talapin, D. V.; Lee, J.-S.; Kovalenko, M. V.; Shevchenko, E. V. *Chem. Rev.* **2009**, *110* (1), 389.
(24) Yeh, C.-Y.; Lu, Z. W.; Froyen, S.; Zunger, A. *Phys. Lett. B* **1992**, *45* (20), 12130.
(25) Pietikainen, J.; S. Laitinen, R. *Chem. Commun.* **1998**, No. 21, 2381.
(26) Thompson, D. P.; Boudjouk, P. *J. Org. Chem.* **1988**, *53* (9), 2109.
(27) Däweritz, L. *Krist. Tech.* **1971**, *6* (1), 101.
(28) Spînulescu-Carnaru, I. *Phys. Status Solidi B* **1966**, *18* (2), 769.
(29) Mitzi, D. B. *Inorg. Chem.* **2005**, *44* (20), 7078.
(30) Li, S.; Yang, G. W. *J. Phys. Chem. C* **2010**, *114* (35), 15054.
(31) Peng, X.; Manna, L.; Yang, W.; Wickham, J.; Scher, E.; Kadavanich, A.; Alivisatos, A. P. *Nature* **2000**, *404* (6773), 59.
(32) Manna, L.; Wang; Cingolani, R.; Alivisatos, A. P. *J. Phys. Chem. B* **2005**, *109* (13), 6183.
(33) Joo, J.; Son, J. S.; Kwon, S. G.; Yu, J. H.; Hyeon, T. *J. Am. Chem. Soc.* **2006**, *128* (17), 5632.
(34) Manna, L.; Scher, E. C.; Alivisatos, A. P. *J. Am. Chem. Soc.* **2000**, *122* (51), 12700.
(35) Bouroushian, M., *Electrochemistry of Metal Chalcogenides*. 1st ed.; Springer: Berlin, Germany, 2010; pp 62−73.
(36) T Mahalingam, V. S. J.; Rajendran, S; Sebastian, P J *Semicond. Sci. Technol.* **2002**, *17* (5), 465.
(37) Steiner, D.; Katz, D.; Millo, O.; Aharoni, A.; Kan, S.; Mokari, T.; Banin, U. *Nano Lett.* **2004**, *4* (6), 1073.
(38) Xie, R.; Zhong, X.; Basché, T. *Adv. Mater.* **2005**, *17* (22), 2741.
(39) Bang, J.; Park, J.; Lee, J. H.; Won, N.; Nam, J.; Lim, J.; Chang, B. Y.; Lee, H. J.; Chon, B.; Shin, J.; Park, J. B.; Choi, J. H.; Cho, K.; Park, S. M.; Joo, T.; Kim, S. *Chem. Mater.* **2009**, *22* (1), 233.
(40) Ying, W.; Andris, S.; John, M.; Edwin, F. H.; Patricia, A. L.; Robert, D. J. *J. Chem. Phys.* **1990**, *92* (11), 6927.
(41) Huang, J.; Huang, Z.; Jin, S.; Lian, T. *J. Phys. Chem. C* **2008**, *112* (49), 19734.